TISSUE ENGINEERING: Part C
Volume 17, Number 2, 2011
© Mary Ann Liebert, Inc.
DOI: 10.1089/ten.tec.2010.0093

Increased Mixing Improves Hydrogel Homogeneity and Quality of Three-Dimensional Printed Constructs

Daniel L. Cohen, Ph.D.,[1] Winifred Lo, B.S.,[1,2] Andrew Tsavaris, B.S.,[1,3] David Peng, M.Eng.,[4] Hod Lipson, Ph.D.,[1,5] and Lawrence J. Bonassar, Ph.D.[1,4]

As the tissue engineering and drug delivery communities place greater emphasis on producing constructs of prescribed geometry and organization, three-dimensional printing is becoming as an increasingly important technique. While numerous tissue printing techniques have emerged, little has been done to characterize the properties of printing inks and the resultant effects on geometric fidelity, cell viability, and mechanical integrity. These questions have been neglected largely because of the lack of methods to characterize the real-time properties of printing inks. We present a novel technique for characterizing the homogeneity of hydrogel tissue printing inks that measures loads during ink deposition and its temporal variation, called, mechanical noise. We then used this technique to determine the effects of increased mixing on the homogeneity of alginate hydrogels and determined whether this results in improved geometric fidelity of printed constructs. We also studied potential adverse effects on cell viability and mechanical integrity of printed parts. Increased mixing between alginate and crosslinker to 128 cycles yielded an 82% reduction in mechanical noise. Geometric fidelity also improved with this increased mixing, in terms of a smoother surface texture, better matching of the target geometry, and fewer point defects. Viability was not adversely affected by increased mixing, and it actually improved by 34% with a 45 min curing time. As mixing before printing was increased from 8 to 200 cycles, the modulus also increased by 110% from 4.0 ± 0.1 to 8.4 ± 1.0 kPa. The results presented herein motivate a radical shift in alginate printing protocol, and also propose a useful methodology for characterizing three-dimensional printing materials.

Introduction

Hydrogels are an increasingly important class of biomaterials for tissue engineering and drug delivery. These materials have long been used for cell delivery in beads,[1,2] disks,[3] and injectable form,[4] and recently their use has been extended to processes such as injection molding[5–11] and three-dimensional (3D) printing.[12–26] Although recently emerging 3D printing applications hold tremendous potential, there are specific challenges associated with using hydrogels for 3D tissue printing. This process requires controlling the sol-gel transition such that the material is sufficiently inviscid while being extruded out of a print nozzle (to preserve mechanical integrity despite shear forces), and yet viscous enough to hold its shape when patterned on a substrate. This process must also preserve cell viability by minimizing shear forces on cells during deposition and avoiding the use of cytotoxic initiators of the sol-gel transition. Toward this end, a number of strategies have been employed including the use of photocrosslinkable (polyethylene glycol[12,19,22]) and thermoreversible (gelatin,[17,18,23–26] pluronic,[21] and collagen[18,20,21]) polymers. Our previous work has used ionically crosslinked alginate hydrogels,[16,25,26] with $CaSO_4$ employed to initiate gelation before material deposition.[14]

Although this process can be used successfully for 3D tissue printing, it is vulnerable to high levels of variability, both within a given print and across consecutive prints. Due to the rapid kinetics of gelation upon contact with calcium, ionic crosslinking of alginate can generate heterogeneous gels,[14,27] which could be detrimental to the tissue printing process. While distribution of calcium ions is a concern that is unique to alginate-based systems, spatial uniformity of crosslinking is likely an issue for all hydrogel-based printing techniques. Such heterogeneity may result from gradients in either chemical crosslinkers or the physical phenomena that induce crosslinking (e.g., heat or light). Although significant heterogeneity

[1]Department of Mechanical and Aerospace Engineering, Cornell University, Ithaca, New York.
[2]Department of Biomedical Engineering, Northwestern University, Evanston, Illinois.
[3]Department of Chemical Engineering, Princeton University, Princeton, New Jersey.
[4]Department of Biomedical Engineering, Cornell University, Ithaca, New York.
[5]Faculty of Computing and Information Science, Cornell University, Ithaca, New York.

has been documented in molded alginate samples,[27] there has been little effort to evaluate the uniformity of printing material or the homogeneity of printed parts. Attempts to conduct such evaluation have been hampered by the lack of methods available for assessing the properties of these hydrogels in real-time during deposition from a print nozzle.

Tissue printing technology has generated much interest due to its ability to generate constructs for a variety of applications ranging from *in vitro* diagnostics to *in vivo* implantation of metabolic or structural tissues. As such, there is no single set of criteria for optimal construct properties (e.g., modulus, diffusivity, and permeability). Regardless of application, it is desirable to have better control of construct composition and organization. A great advantage of tissue printing technologies is the potential to exert such control through the processes by which printing inks are formulated and deposited.

One particularly important process parameter, perhaps most pertinent to the homogeneity of the resultant gels, is the amount of mixing used to combine the alginate and crosslinker solutions before printing. This poorly understood process parameter was never studied in a 3D printing context. Previously, eight mixings through as stopcock was thought to be sufficient for 3D printing gels (a process inherited from the technique's injection molding heritage[5–11]), but this idea has never been tested.

The goals of this study were twofold: (1) to develop a quantitative method for characterizing hydrogel homogeneity during printing, and (2) to use this technique to determine whether increased mixing improved gel homogeneity and geometric fidelity of printed parts, while preserving cell viability and mechanical integrity. We present a novel characterization technique that measures extrusion force in real-time during deposition and describes gel homogeneity in terms of the extrusion force temporal variation, called mechanical noise. In addition to determining the effects of mixing on gel homogeneity, we used visual inspection to determine the effects of mixing on geometric fidelity of printed parts. We also used the Live/Dead assay and confined compression mechanical testing to determine whether gel homogeneity benefits came at the expense of cell viability and mechanical integrity, respectively.

Materials and Methods

Cell isolation

Chondrocytes were isolated from articular cartilage obtained from the femeropatellar groove of 1- to 3-day-old calves, as described previously.[28] The tissue was digested for 18 h at 37°C and 5% CO_2 in Dulbecco's modified Eagle's medium containing 0.3% collagenase. The digest solution was filtered with a 100 μm cell strainer. The articular chondrocytes were isolated from the strained digest solution by centrifugation at 412 *g* for 7 min. Cells were washed twice with phosphate-buffered saline (PBS). The initial viability was determined using trypan blue (Mediatech, Herndon, VA), and only batches of cells with viability of >90% were used.

Alginate hydrogel formulation and cell encapsulation

Alginate hydrogels for cell printing were prepared using techniques based on those described previously.[14] In this approach, alginate and calcium solutions are combined, and through ionic crosslinking a gel is formed. A multilayered construct can be printed with the material since the reaction rate is sufficiently slow to allow for partially uncrosslinked alginate to bond with subsequently deposited alginate/calcium.[29,30] The alginate was prepared by mixing low-viscosity, high G-content nonmedical-grade LF10/60 alginate (FMC Biopolymer, Drammen, Norway) with PBS at a concentration of 20 mg/mL. For experiments requiring cell-seeded gels, cells were mixed into the alginate solution using a vortex spinner at a density of 50 million cells/mL before mixing with the crosslinker. The $CaSO_4$ crosslinker was prepared at a concentration of 10 mg/mL in PBS. The alginate and crosslinker were combined in a 2:1 ratio by volume and then mixed a variable number of times (from 8 to 200 times, depending on the experiment) through a stopcock at 1 Hz. The mixed alginate hydrogel was loaded into a syringe and allowed to cure for 15–45 min before use in any printing or experimentation.

Solid freeform fabrication system

A Fab@Home open-source, open-architecture solid freeform fabrication system was used for printing of the hydrogel[31] (Fig. 1). This system, which was designed and deployed by our lab, comprised a laser cut acrylic base with a three-axis gantry motion system. Each axis was belt-driven and actuated by a stepper motor (Haydon Switch & Instruments, Waterbury, CT). Communication and motion was coordinated by a universal serial bos (USB)-interfaced electronic control board based on the Olimex LPC-H2148 microcontroller. The open-source control software was written by our lab, and along with the hardware design files, are freely available at www.fabathome.org. This software imported CAD models in stereolithography (STL) file format, sliced the geometries layer-wise and planned tool paths for each layer based upon user-specified printing parameters. The standard printing parameters used in the following experiments were 0.68 mm path width, 0.68 mm path height, and 10 mm/s gantry traverse rate. Software also communicated with the control board and was responsible for coordinating motion among the gantry axes and the deposition tool.

The standard Fab@Home deposition tool was modified to accommodate sterile syringes for biological applications. The deposition tool gripped 10 mL disposable syringes (Exel International Medical Products, St. Petersburg, FL) and pushed upon the syringe plunger with a stepper motor at 0.25 mm/s (Fig. 1). Tapered Luer-lok syringe tips (EFD Inc., East Providence, RI) of 0.25 mm inner diameter were attached to the syringe barrel and were used as the nozzle. For experiments utilizing cells, each tip was sterilized in 70% isopropyl alcohol for 2 h.

Measurement of gel homogeneity

Gel homogeneity was assessed by measuring the real-time extrusion force variation during deposition. With a perfectly homogenous deposition material, if a constant displacement rate were imposed on the syringe plunger, the uniformity of the material would yield a constant extrusion force. That is, the force required to achieve the target constant displacement rate would also be constant, and the magnitude would depend on the displacement rate, material viscosity, and

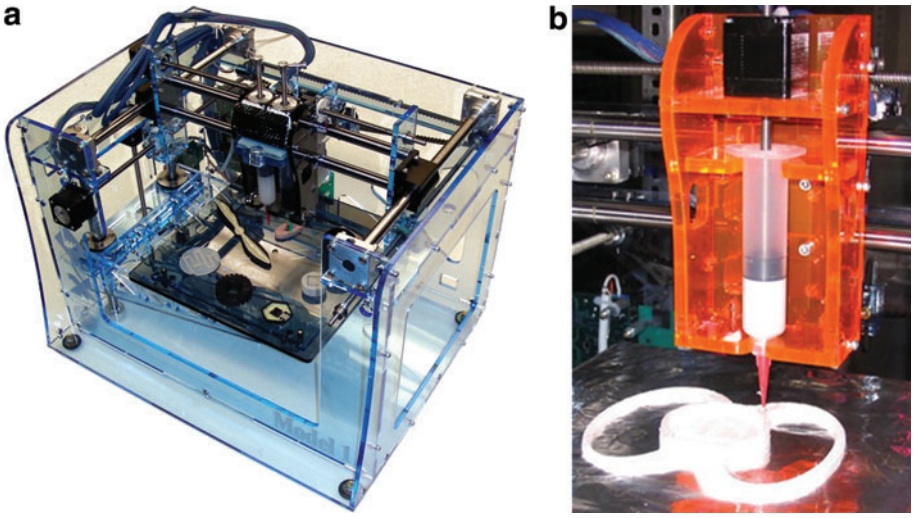


FIG. 1. Fab@Home open-source open-architecture three-dimensional printing system. **(a)** Hardware comprising three-axis gantry motion system and deposition tool. **(b)** The material-filled syringes plug into the Fab@Home's deposition tool, and a stepper motor pushes upon the plunger to extrude material through the Luer-lok deposition tip. Color images available online at www.liebertonline.com/ten.

orifice diameter. By contrast, if the deposition material were compositionally heterogeneous, as portions of varying the extent of crosslinking passed through the syringe tip, the force required to maintain a constant plunger displacement rate would vary. More specifically in the case of alginate hydrogel deposition, as clumps of over-crosslinked gel attempted to pass through the syringe tip at a constant displacement rate, the clumps' relatively the extent of crosslinking would cause the plunger extrusion force to increase; conversely, as under-crosslinked clumps passed through the syringe tip, the plunger extrusion force would decrease. Gels with greater compositional heterogeneity would exhibit greater temporal variation of the plunger extrusion force. This temporal variation in plunger extrusion force can be quantitatively represented by calculating the standard deviation of the plunger extrusion force over time. Herein, we call the standard deviation of the plunger extrusion force over time, mechanical noise.

A novel experimental platform was devised to measure the mechanical noise exhibited by alginate hydrogels during prints. We needed to precisely measure the plunger extrusion forces that typically occur within a deposition tool. Toward this end, the syringe was held within a custom jig (Fig. 2) that was mounted on an ELF3200 mechanical test-frame (EnduraTec, Minnetonka, MN). The jig was mounted to the static bottom plate of the test-frame and held the syringe vertically, similar to how the deposition tool houses the syringe. The mechanical test-frame's top plate was actuated and capable of being driven at constant displacement rates. A 50 lb load cell (Sensotec, Columbus, OH) was mounted to the top plate of the test-frame and also connected to the syringe plunger via a custom adapter (Fig. 2). The test-frame's actuated top plate behaved analogously to the stepper motor of the deposition tool, in that both imposed constant displacement rates onto the syringe plunger. The test-frame's top plate was displaced at 0.25 mm/s (the same linear rate as the deposition tool's stepper motor) to reproduce the syringe plunger extrusion rates that occur during printing; meanwhile, the in-line load cell collected force data at 200 Hz. The forces reproduced in the test-frame were highly representative of typical 3D printing scenarios since the extrusion rates were identical and the same wetted components (i.e., 10 mL Exel syringes and 0.25-mm-diameter EFD syringe tips) were used in both systems. For these mechanical noise measurements, non-cell-seeded gels were prepared according to the protocol described above, and the extent of mixing was prescribed between 8 and 200 mixings.

To accurately describe the mechanical noise of the gel, two types of noise needed to be filtered out from the raw plunger extrusion force data. First, very high-frequency plunger extrusion force variation appeared to be a result of plunger-on-syringe wall friction (Fig. 3). This high-frequency noise was determined to be nonmaterial specific plunger-on-syringe friction because it was also present in tests performed with water. It was clear from these calibration experiments that the high-frequency component of the plunger extrusion force variation was not related to the deposition material heterogeneity. A second type of noise that needed to be filtered out was very low-frequency variation that was related to the taper of the syringe barrel. For practical reasons related to the injection molding process by which the syringes were manufactured, most commercial syringes are designed with a 1° taper, called the draft. Consequently, as the plunger moved deeper into the syringe barrel, the diameter decreased and the plunger-on-syringe wall friction increased, which ultimately increased the plunger extrusion force. Again, this low-frequency phenomenon was also present in tests with water as the deposition material, and it was clear that the effect was unrelated to material heterogeneity.

The high-frequency friction and low-frequency draft effects were both removed so that the resultant extrusion force variation would be purely indicative of the material heterogeneity. To do so, a band-pass filter was applied to the plunger extrusion force. Force variations between the frequencies of 0.5 and 40 Hz were passed; these threshold values were determined experimentally by using water as a calibration deposition material due to its low viscosity and high homogeneity. Finally, the mechanical noise was calculated as the standard deviation of the band-pass-filtered plunger extrusion force over 25 s, with the first 5 s disregarded.

Statistically significant differences were analyzed using a one-way analysis of variance (ANOVA), *post-hoc* Tukey test, with a p-value of 0.05.

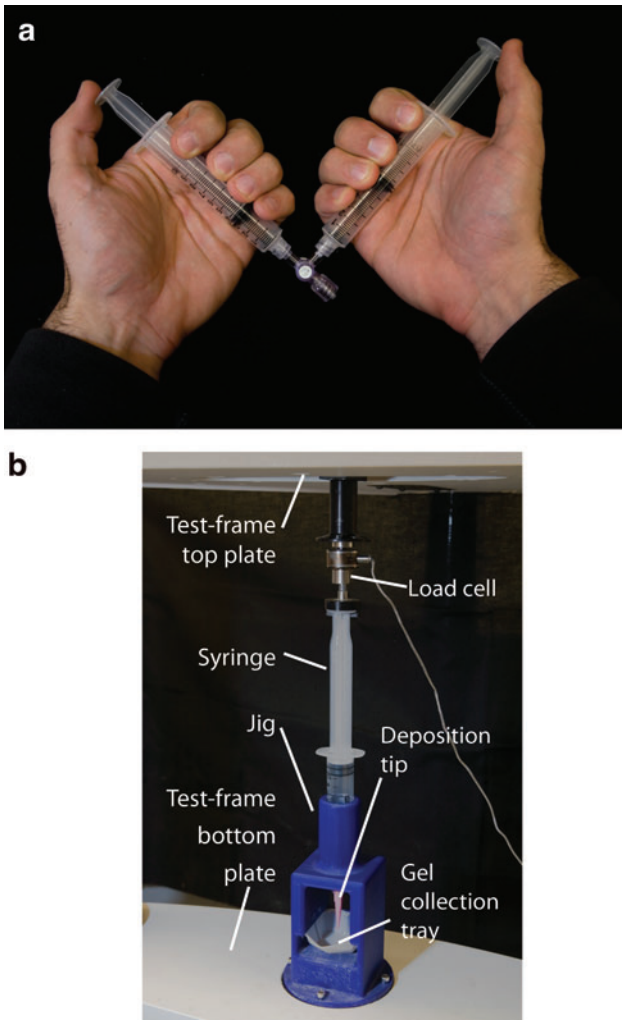


FIG. 2. Gel homogeneity characterization platform. **(a)** Gels are mixed by manually pumping alginate and crosslinker solutions through a three-way stopcock at 1 Hz for a variable number of cycles, depending on the experiment. **(b)** For gel characterization, the syringe is held vertically by the custom jig and material is extruded through the deposition tip into a disposable weigh boat, which serves as a collection tray. An in-line load cell measures the plunger extrusion force in real-time during deposition. The mechanical test-frame imposes a displacement at a constant rate and measures the plunger extrusion force with a 50 lb load cell at 200 Hz. Color images available online at www.liebertonline.com/ten.

Geometric fidelity characterization

Geometric fidelity was qualitatively characterized by visually inspecting constructs printed on the Fab@Home solid freeform fabrication system. Computer-aided design (CAD) models of various geometries were converted into STL files and loaded into the Fab@Home control software, including high-aspect ratio cylinders, cubes, disks, and an ovine meniscus from CT imaging. Software subsequently planned the tool paths and afterward, non-cell-seeded alginate gel was mixed between 8 and 200 times, loaded into syringes, and placed in the deposition tool. The gel preparation and prints were conducted according to the protocol described above.

Photographs of the printed constructs were captured for subsequent comparison between samples of different test groups. Key characteristics emphasized during observation included surface texture, similarity of the overall shape compared to the intended geometry, and presence of point defects such as missing material.

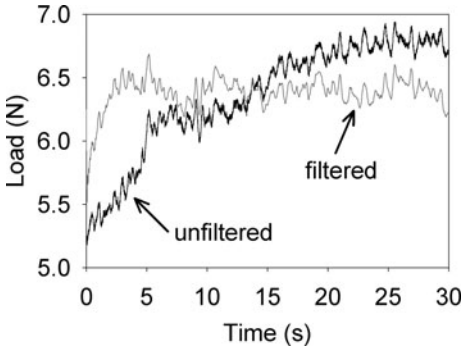


FIG. 3. Effects of band-pass filtering. The dark black line represents raw plunger extrusion force versus time for a 200 cycle-mixed gel through a tip of 0.25 mm diameter at a constant plunger displacement rate of 0.25 mm/s. The 1° draft tapering within the syringes causes the mean running-average-load to monotonically increase. The dark gray line represents the band-pass-filtered load, where frequency components below 0.5 Hz and above 40 Hz were removed (to account for the draft and plunger-on-syringe friction). While transient effects are still present during the first ~5 s of the filtered load resulting from the ramp-up of the test-frame, the load reaches a steady state in which the running-average-load no longer monotonically increases.

Elastic modulus characterization

Using the hydrogel fabrication protocol described above, non-cell-seeded alginate hydrogel was mixed between 8 and 200 times, and subsequently cast between glass plates using 1 mm spacer plates. Disks were stamped out with a 6-mm-diameter biopsy punch, postcrosslinked for 20 min in 2% $CaCl_2$, and stored for no >1 h in HEPES buffer. The disks were then placed in an ELF 3200 (EnduraTec) mechanical test-frame in a confined compression chamber to assess equilibrium modulus as described previously.[32] A 1000 g load cell (Sensotec) with 2 g resolution was attached to the bottom plate and a displacement sensor to the top plate. The bottom plate was filled with PBS to completely encompass the sample with fluid. The two plates started at a distance corresponding to 0% strain and stepped 0.1 mm toward each other every 100 s until 45% strain was achieved. Load data were acquired at a frequency of 5 Hz, and displacement and load data were converted to strain and stress, respectively, by normalizing to sample thickness and area. The stress–strain curve of each printed sample was analyzed by first finding the equilibrium stress corresponding to each imposed strain (0%–45%). The linear region of the equilibrium stress–strain curve was fit linearly; the slope of this line was the Young's modulus of the sample.

Statistically significant differences were analyzed using a one-way ANOVA, *post-hoc* Tukey test, with a p-value of 0.05.

Viability test

Viability of the cells suspended in the alginate gel was measured immediately after the printing process. Disks,

6 mm in diameter×2 mm in height, were printed on the Fab@Home using the same gel preparation and printing protocol described above. Gels were mixed between 8 and 200 times. In addition to the standard syringe tip diameter of 0.25 mm, diameters of 0.61 and 5 mm were also used during viability experimentation. Also, in addition to the standard duration of 15 min between mixing and printing, 30 and 45 min curing periods were also tested with a 0.25-mm-diameter tip. During material curing, the samples were exposed to room temperature conditions. Each sample was tested with the Live/Dead Viability Assay (Molecular Probes, Eugene, OR). The samples were exposed to 0.15 μM calcein AM and 2 μM ethidium homodimer-1 for 60 min at room temperature. The stained samples were analyzed under a Nikon TE2000-S microscope equipped with an epifluorescence attachment and a Spot RT digital camera. The viability was calculated as the average of the ratios of live over total cells in a hemacytometer (Hausser Scientific, Horsham, PA), normalized by the initial cell viability.

Statistically significant differences were analyzed using a two-way ANOVA, *post-hoc* Tukey test, with a *p*-value of 0.05. All data are presented as mean ± standard error of the mean.

Results

Effects of mixing amount on gel homogeneity

Gels that were prepared with greater mixing of the alginate and crosslinker before printing exhibited much less temporal variation in plunger extrusion force. That is, for samples that were highly mixed, the max-to-min variation in extrusion force was smaller than for those samples that were mixed fewer times (Fig. 4). Gels that were mixed eight times exhibited a load of ~1.5 N, whereas gels mixed 200 times only exhibited ~0.5 N.

The effect of mixing amount on gel homogeneity was also apparent when expressed in terms of mechanical noise, or the standard deviation of the plunger extrusion force over time (Fig. 5). For samples mixed eight times, the mechanical noise was 0.77 ± 0.16 N ($n = 10$). The mechanical noise drastically dropped to 0.25 ± 0.05 N at 16 mixings ($p < 0.05$) and continued to drop to 0.14 ± 0.01 N at 128 mixings ($n = 10$). In the low-mixing regime, merely increasing the mixing by eight cycles yielded a 68% reduction in mechanical noise. The additional mixing cycles between 16 and 128 mixings yielded an additional 44% reduction in mechanical noise. Overall, mixing 128 times instead of 8 times yields an 82% decrease in mechanical noise ($p < 0.05$).

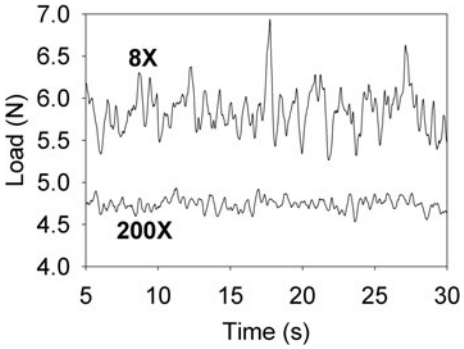


FIG. 4. Heterogeneity of gel reflected in temporal load. The two lines represent band-pass-filtered temporal load, of which the first 5 s have been discarded to ignore transients resulting from test-frame ramp-up. The 200 cycle-mixed gel exhibits much narrower temporal variation in load, with a range of ~0.5 N, whereas the 8 cycled-mixed gel exhibits a range of ~1.5 N.

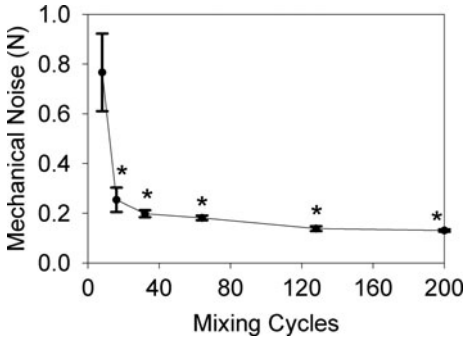


FIG. 5. Mechanical noise versus number of mixing cycles. As the number of mixing cycles between the alginate and crosslinker increases from 8 to 200 cycles, the associated mechanical noise monotonically decreases. At 8 mixing cycles, the mechanical noise is 0.77 ± 0.16 N, and as the mixing cycles increases to 120 cycles, the mechanical noise drops by 82% to 0.14 ± 0.01 N. Error bars represent the standard error of the mean and $n = 10$; $^*p < 0.05$ versus eight mixings.

Effects of mixing amount on geometric fidelity of printed constructs

Geometric fidelity was qualitatively assessed in terms of surface texture, similarity to target geometry, and point defects. Samples that were printed with gels mixed 200 times exhibited much smoother surfaces than those mixed only 8 times. Further, the 200× samples exhibited closer similarity to the target geometry and fewer point defects, such as locations with missing material or too much material.

The higher geometric fidelity of 200× printed gels, as compared to 8× gels, was particularly evident in the print of the ovine meniscus from CT imaging (Fig. 6). The surface texture of the 8× sample was rougher and clearly displayed the laminar nature of the layer-wise manufactured construct. However, the 200× sample had a smooth surface and the individual layers were visually imperceptible.

Further, the 200× samples better matched the intended geometry particularly at the horns of the meniscus and alone the top rim of the construct. As for point defects, the 8× sample exhibited numerous cavities of missing material as well as mounds of gel that are nonexistent in the target geometry.

Not only was within-print geometric fidelity higher for 200× gels, but also the print-to-print variability was much smaller (Fig. 6). The 200× gels yielded constructs that were consistently smooth, defect free, and similar to the target geometry. However, the geometric fidelity of 8× gels greatly varied from print-to-print, sometimes yielding prints of moderate geometric fidelity but other times yielding very poor geometric fidelity.

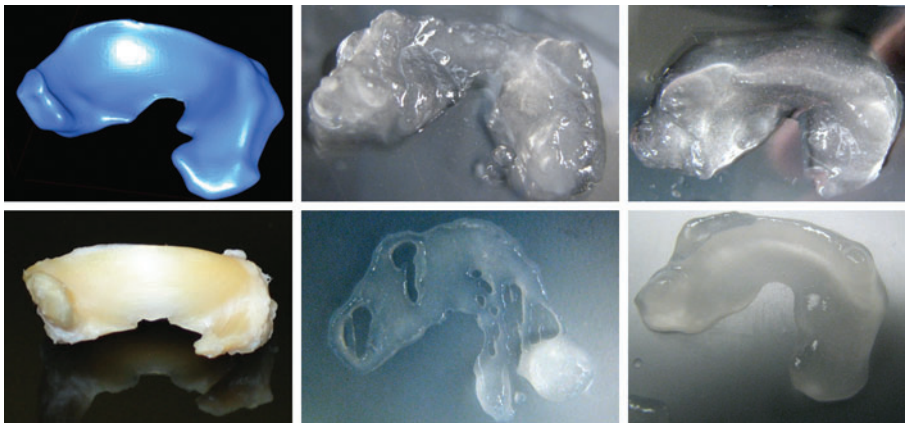


FIG. 6. Geometric fidelity of printed ovine menisci versus number of mixing cycles. An ovine meniscus (bottom-left) was imaged using a computed tomography scanner (top-left) and printed. The print with the eight cycle-mixed gel (top-middle) exhibited a rough surface texture, presence of point defects including cavities, and deviation from target geometry along the upper rim. The print with the 200× gel (top-right) exhibited a smoother surface texture, better matching of the target geometry, and fewer point defects. Also, print-to-print variability was poorer with the 8× gel, sometimes resulting in complete failures (bottom-middle), whereas the 200× gel produced more consistent results (bottom-right). Color images available online at www.liebertonline.com/ten.

Effects of mixing amount on elastic modulus of printing gel

The compressive modulus of hydrogel disks increased monotonically with mixing (Fig. 7). At 30 mixings, the postcrosslinked printed disks possessed an elastic modulus of 4.0 ± 0.1 kPa ($n = 5$). The elastic modulus increased to 5.9 ± 0.3 kPa and 8.4 ± 1.0 kPa, at 120 and 200 mixing cycles, respectively ($n = 5$). The fourfold increase in mixing between 30 and 120 cycles yielded a 50% increase in elastic modulus ($p < 0.05$). Overall, mixing the gel 200 times versus only 30 times yielded a 110% increase in elastic modulus ($p < 0.05$).

Effects of mixing amount on viability of printed constructs

The first viability experiment tested the effect of tip diameter, from 0.25 to 5 mm, on viability with samples that were printed 15 min after mixing under various mixing techniques, including 8×, 64×, and 200×. While the viabilities ranged from 65% to 77%, it did not do so as a function of tip diameter or number of mixing cycles (Fig. 8).

The second viability experiment tested the effect of cure time (i.e., the time between mixing and printing) on viability. For gels printed through a 0.25-mm-diameter tip, 8× and 200× gels did not have different viabilities with cure times of 15 min nor of 30 min. However, with a cure time of 45 min, the viability increased ($p < 0.05$) for 200× gels compared to 8× gels (Fig. 9). With a 45 min cure time, printed 8× gels only had a viability of $64.5\% \pm 5.1\%$. However, printed 200× gels had a 34% higher viability, $87.1\% \pm 2.4\%$.

Discussion

This study is one of the first to present a method for assessing the printing characteristics, in particular, the homogeneity, of tissue printing inks. A mechanical test-frame was used to capture load data during extrusion of alginate hydrogel through a deposition nozzle. The load data were filtered to remove friction effects unrelated to the hydrogel, and the standard deviation of the temporal syringe extrusion force was taken as the mechanical noise of the gel. Standard

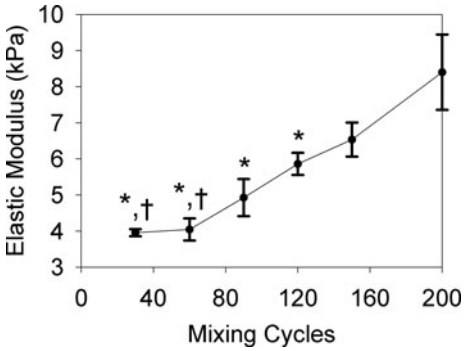


FIG. 7. Elastic modulus versus number of mixing cycles. As the number of mixing cycles between the alginate and crosslinker increases, from 30 to 200 cycles, the associated elastic modulus monotonically increases. At 30 mixing cycles, the mechanical noise is 4.0 ± 0.1 N and as the mixing cycles increases to 200 cycles, the mechanical noise increases by 110% to 8.4 ± 1.0 N. Error bars represent the standard error of the mean and $n = 5$; $^{*}p < 0.05$ versus 200 mixings and $^{\dagger}p < 0.05$ versus 150 mixings.

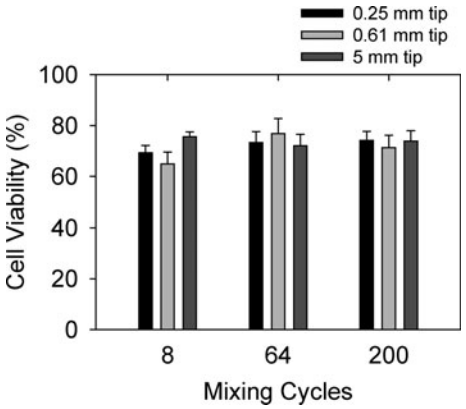


FIG. 8. Cell viability versus deposition tip diameter and number of mixing cycles. The size of the deposition tip, within the range of 0.25–5 mm, does not have effect on the viability of printed cells. Error bars represent the standard error of the mean and $n = 10$.

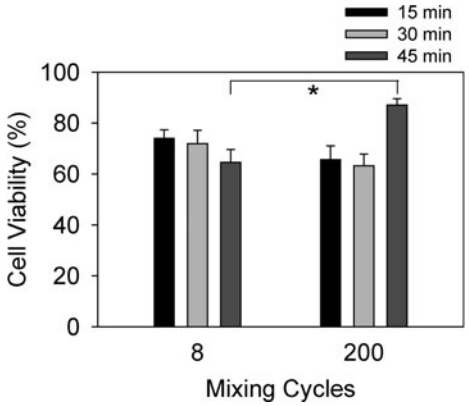


FIG. 9. Cell viability versus time between mixing and printing, and number of mixing cycles. Viability does not significantly vary with mixing at cure times of 15 or 30 min. However, with a cure time of 45 min, the viability increases by 34% from 64.5% ± 5.1% in an 8× gel to 87.1% ± 2.4% in a 200× gel. Error bars represent the standard error of the mean and $n = 10$; $^*p < 0.05$.

material characterization techniques, such as measurement of elastic modulus and viscosity, do not serve as good indicators of how a gel will behave during printing since the gel likely comprises both solid and liquid components in unknown, and possibly changing, proportions. Further, these test methods fail to accurately describe a gel's printability due to the printing technique's extreme sensitivity to heterogeneity of the printing ink. Due to the rapid kinetics of gelation when calcium is mixed with alginate, these hydrogels are highly susceptible to localized variation in material properties. As portions of varying crosslinking extents are pushed through the deposition tool at constant displacement rates, these variations in gel properties lead to inconsistent flow rates that adversely affect the geometric fidelity of printed parts; in extreme cases, the printer will completely clog as over-crosslinked clumps attempt to pass through the deposition tool.

Unlike traditional material characterization methods, the technique presented herein not only describes the homogeneity of printing inks, but also does so directly in a 3D printing context. That is, gel homogeneity was measured within the same types of wetted components (i.e., syringes and syringe tips) that are used in 3D printers and the forces imposed on the syringes mimic those during an actual print. This measurement within a 3D printing context enhances the usefulness of the results obtained because the test conditions so closely match those of the end-use; consequently, the methodology is highly relevant for characterizing positive displacement extrusion of hydrogels,[14,15,21] as well as non-hydrogel biomaterials.[33,34] This characterization methodology is also applicable to characterization of bioprinting inks for pressure deposition[13,17,18,23–26,35–39] and rotary screw extrusion[40–42] techniques, even though the printing apparatus' configurations are not identical to the experimental setup.

Mixing had a profound effect on the homogeneity of alginate gel during printing. Mixing 16 cycles versus the established 8-cycle norm yielded a 68% decrease in mechanical noise. Further, mixing 128 cycles versus 8 cycles delivers an 82% reduction in mechanical noise. Such high mixing cycles were completely at odds with the established injection molding protocol,[5–11] which considered 128 or even 16 mixing cycles entirely unnecessary and detrimental to the viability and mechanical integrity of resultant constructs.

Increased mixing of the alginate and calcium crosslinker enhanced gel homogeneity due to the more thorough redistribution of the calcium ions. As the gel is further mixed, the additional mixing energy more evenly distributed the calcium ions throughout the calcium-alginate mixture. With more even calcium ion distribution, the local concentration of calcium is more uniform and the resultant crosslinking extent of the gel is likewise more consistent. In poorly mixed gels, uneven calcium ion concentration leads to localized pockets of under- and over-crosslinked gel, which result in varying flow rates when a constant displacement rate is imposed on the syringe plunger.

While average homogeneity increases with mixing, it appears that so too does the variability in homogeneity from sample to sample. Depending on the specific application, one may need to weigh trade-offs and determine whether average homogeneity or variability in homogeneity is more important as he or she chooses a mixing technique.

We next needed to determine whether the improved homogeneity of the alginate gel translated to improvements in geometric fidelity of printed constructs. Prints conducted with 200× gels indeed exhibited smoothers surfaces, less perceptible layering, closer matching to target geometry, and fewer point defects than prints conducted with 8× gels. Further, 200× gels yielded better print-to-print reliability in terms of geometric fidelity. That is, 200× gels consistently produced constructs of high geometric fidelity, whereas 8× gels resulted in a much wider range of geometric fidelities, varying from moderate to very poor.

Increased mixing improved geometric fidelity likely because the greater homogeneity led to more consistent deposition flow rates. The geometric fidelity of printed constructs is highly sensitive to the uniformity of the deposition material flow. Since the deposition tool traverses without feedback on the material flow, even slight changes in the material flow rate load to cavities if the flow rate is too low or mounds if the rate is too high. In extreme cases, the gel heterogeneity leads to over-crosslinked clumps of gel attempting to pass through the deposition tool, in which case the tool completely clogs and deposition halts entirely.

Even though we demonstrated the gel homogeneity and geometric fidelity benefits of increased mixing, we still needed to address the concerns that such mixing would adversely affect viability and mechanical integrity. While mechanical properties[43] and viability[44,45] of printed hydrogel constructs have been studied, they have never been analyzed as a function of mixing technique and gel homogeneity. We employed elastic modulus mechanical testing and the Live/Dead assay to investigate the effects of increased mixing to rule out potential adverse effects.

One concern was that mixing beyond four to eight cycles would degrade the mechanical integrity of the resultant gel because as the gel mixes it transitions into a solid, and further mixing would permanent rip the material. Our testing demonstrated that rather than degrading mechanical integrity, increased mixing actually increased the final elastic modulus twofold. Mixing 120 times instead of 30 times increased the final elastic modulus 50% to 5.9 kPa. Increasing

the mixing from 30 to 200 cycles yields a 110% increase in the final elastic modulus of the printed constructs, resulting in a modulus of 8.4 kPa. Interestingly, although we were initially concerned about detrimental shearing of the gel through increased mixing, we did not observe such effects and instead actually saw enhanced mechanical integrity resulting from increased mixing. Several hypotheses potentially explain why increased mixing improved mechanical integrity. First, better distribution of the calcium ions initially as the gel was mixed may have made the ions more readily available for crosslinking through the constructs resulting in more efficient use of the ions. Second, better distribution of the calcium may have eliminated pockets of extremely over-crosslinked gel, which upon deposition would have been torn apart by the restricted orifice of the deposition tool to the detriment of the overall mechanical integrity. Third, by eliminating these localized pockets of over-crosslinked gel, the gel may have exhibited more consistent diffusivity, which further allowed for efficient transport and use of calcium ions, as well as allowed for polymer chain realignment. It should be noted that the disks used for mechanical property characterization were postcrosslinked in $CaCl_2$ as described above, and although this is a valid postprocessing option that could be chosen depending on context, for certain applications it may not be necessary to further increase the elastic modulus. If postcrosslinking is employed, attention must be paid to the potential effects it could have on the homogeneity of printed constructs. In the mechanical property testing, the disks were likely sufficiently small such that the postcrosslinking did not introduce substantial heterogeneities. For larger prints, however, future work should determine precisely what effect postcrosslinking would have on construct homogeneity.

Besides mechanical integrity being preserved, we also found that viability of the cells within printed constructs was maintained even with increased mixing. Not only was cell viability preserved over a range of syringe tip diameters, but also, when a print was conducted 45 min after mixing, the viability of 200× gels was actually statistically significantly higher than for 8× gels. We believe that as mixing is increased, the gel becomes more homogenous and localized clumps of over-crosslinked gel are eliminated. These clumps, present in less mixed samples, exert high shear stress on the cells when forced through the nozzle and consequently decrease sample viability.[44] We also believe that this effect is only noticeable with a curing time of 45 min, and not with lesser curing times, because the overall crosslinking extent of the gel is too low in lesser cured samples for the clumps to exert shear stresses above the critical threshold.

It is important to note that 3D printing has many applications, from implant generation to diagnostics to 3D culture. There is consequently no single set of desired cell-hydrogel properties as the required modulus, viability, geometric fidelity, and homogeneity are entirely dependent on context. The work presented herein explores some of the important process variables so that end-users can weigh the trade-offs and choose the process parameters that meet their specific needs.

Conclusion

This study not only provides greater insight into the effects of mixing on alginate hydrogel properties, but also fundamentally changes key process parameters that drastically improve the efficacy of hydrogel 3D printing. Instead of relying upon established guidelines of 4–8 mixings,[5–11] we suggest a radical shift to a mixing regime of 128–200 mixings. We also have proven that such a radical shift in technique does not come at the expense of mechanical properties or cell viability and, to the contrary, actually improves both aspects. In addition to improving alginate hydrogel 3D printing, we also provide a test methodology that enables the characterization all hydrogels,[12–26] as well as other types of biologically relevant printing inks.[33–42] The test methodology is directly applicable to positive displacement-based printing techniques, but is also useful for characterizing pressure-based[13,17,18,23–26,35–39] and rotary screw-based[40–42] printing approaches. As tissue 3D printing moves closer toward the clinic, we will need to address concerns about reliability, and methodologies such as the one presented herein are crucial for optimizing printing inks and ensuring acceptable levels of reproducibility.

Acknowledgments

The authors would like to acknowledge the support of the Cornell Center for Material Research Undergraduate Experience Program (NSF Grant DMR 0520404), as well as the NSF Graduate Research Fellowship Program.

Disclosure Statement

No competing financial interests exist.

References

1. Beekman, B., Verzijl, N., Bank, R.A., Mark, K.V.D., and TeKoppele, J.M. Synthesis of collagen by bovine chondrocytes cultured in alginate: posttranslational modifications and cell-matrix interaction. Exp Cell Res **237,** 135, 1997.
2. Enobakhare, B.O., Bader, D.L., and Lee, D.A. Quantification of sulfated glycosaminoglycans in chondrocyte/alginate cultures, by use of 1,9-dimethylmethylene blue. Anal Biochem **243,** 189, 1996.
3. Paige, K.T., Cima, L.G., Yaremchuk, M.J., Schloo, B.L., Vacanti, J.P., and Vacanti, C.A. *De novo* cartilage generation using calcium alginate-chondrocyte constructs. Plast Reconstr Surg **97,** 168, 1996.
4. Paige, K.T., Cima, L.G., Yaremchuk, M.J., Vacanti, J.P., and Vacanti, C.A. Injectable cartilage. Plast Reconstr Surg **96,** 1390, 1995.
5. Ballyns, J.J., Cohen, D.L., Malone, E., Maher, S.A., Potter, H.G., Wright, T.M., Lipson, H., and Bonassar, L.J. An optical method for evaluation of geometric fidelity for anatomically shaped tissue engineered constructs. Tissue Eng Part C Methods **16,** 693, 2010.
6. Ballyns, J.J., Gleghorn, J.P., Niebrzydowski, V., Rawlinson, J.J., Potter, H.G., Maher, S.A., Wright, T.M., and Bonassar, L.J. Image-guided tissue engineering of anatomically shaped implants via MRI and micro-CT using injection molding. Tissue Eng Part A **14,** 1195, 2008.
7. Chang, S.C., Rowley, J.A., Tobias, G., Genes, N.G., Roy, A.K., Mooney, D.J., Vacanti, C.A., and Bonassar, L.J. Injection molding of chondrocyte/alginate constructs in the shape of facial implants. J Biomed Mater Res **55,** 503, 2001.
8. Chang, S.C., Tobias, G., Roy, A.K., Vacanti, C.A., and Bonassar, L.J. Tissue engineering of autologous cartilage for

craniofacial reconstruction by injection molding. Plast Reconstr Surg **112,** 793, 2003.
9. Hott, M.E., Megerian, C.A., Beane, R., and Bonassar, L.J. Fabrication of tissue engineered tympanic membrane patches using computer-aided design and injection molding. Laryngoscope **114,** 1290, 2004.
10. Kuo, C.K., and Ma, P.X. Maintaining dimensions and mechanical properties of ionically crosslinked alginate hydrogel scaffolds *in vitro*. J Biomed Mater Res Part A **84,** 899, 2008.
11. Xu, J.-W., Zaporojan, V., Peretti, G.M., Roses, R.E., Morse, K.R., Roy, A.K., Mesa, J.M., Randolph, M.A., Bonassar, L.J., and Yaremchuk, M.J. Injectable tissue-engineered cartilage with different chondrocyte sources. Plast Reconstr Surg **113,** 1361, 2004.
12. Albrecht, D.R., Tsang, V.L., Sah, R.L., and Bhatia, S.N. Photo- and electropatterning of hydrogel-encapsulated living cell arrays. Lab Chip **5,** 111, 2004.
13. Ang, T.H., Sultana, F.S.A., Hutmacher, D.W., Wong, Y.S., Fuh, J.Y.H., Mo, X.M., Loh, H.T., Burdet, E., and Teoh, S.H. Fabrication of 3D chitosan-hydroxyapatite scaffolds using a robotic dispensing system. Mater Sci Eng Part C **20,** 35, 2002.
14. Cohen, D.L., Malone, E., Lipson, H., and Bonassar, L.J. Direct freeform fabrication of seeded hydrogels in arbitrary geometries. Tissue Eng **12,** 1325, 2006.
15. Geng, L., Feng, W., Hutmacher, D.W., Wong, Y.S., Loh, H.T., and Fuh, J.Y. Direct writing of chitosan scaffolds using a robotic system. Rapid Prototyping J **11,** 90, 2005.
16. Khalil, S., and Sun, W. Bioprinting endothelial cells with alginate for 3D tissue constructs. J Biomech Eng **131,** 1002, 2009.
17. Landers, R., Hübner, U., Schmelzeisen, R., and Mülhaupt, R. Rapid prototyping of scaffolds derived from thermoreversible hydrogels and tailored for applications in tissue engineering. Biomaterials **23,** 4437, 2002.
18. Landers, R., Pfister, A., Hübner, U., John, H., Schmelzeisen, R., and Mülhaupt, R. Fabrication of soft tissue engineering scaffolds by means of rapid prototyping techniques. J Mater Sci **37,** 3107, 2002.
19. Lu, Y., Mapili, G., Suhali, G., Chen, S., and Roy, K. A digital micro-mirror device-based system for the microfabrication of complex, spatially patterned tissue engineering scaffolds. J Biomed Mater Res Part A **77,** 396, 2006.
20. Mironov, V., Boland, T., Trusk, T., Forgacs, G., and Markwald, R.R. Organ printing: computer-aided jet-based 3D tissue engineering. Trends Biotechnol **21,** 157, 2003.
21. Smith, C.M., Stone, A.L., Parkhill, R.L., Stewart, R.L., Simpkins, M.W., Kachurin, A.M., Warren, W.L., and Williams, S.K. Three-dimensional BioAssembly tool for generating viable tissue-engineered constructs. Tissue Eng **10,** 1566, 2004.
22. Tsang, V.L., and Bhatia, S.N. Three-dimensional tissue fabrication. Adv Drug Delivery Rev **56,** 1635, 2004.
23. Wang, X., Yan, Y., Pan, Y., Xiong, Z., Liu, H., Cheng, J., Feng, L., Feng, L., Wu, R., Zhang, R., and Lu, Q. Generation of three-dimensional hepatocyte/gelatin structures with rapid prototyping system. Tissue Eng **12,** 83, 2006.
24. Wei, X., Xiaohong, W., Yongnian, Y., Wei, Z., Zhuo, X., Feng, L., Rendong, W., and Renji, Z. Rapid prototyping three-dimensional cell/gelatin/fibrinogen constructs for medical regeneration. J Bioactive Compatible Polym **22,** 363, 2007.
25. Yan, Y., Wang, X., Pan, Y., Liu, H., Cheng, J., Xiong, Z., Lin, F., Wu, R., Zhang, R., and Lu, Q. Fabrication of viable tissue-engineered constructs with 3D cell-assembly technique. Biomaterials **26,** 5864, 2005.
26. Yan, Y., Wang, X., Xiong, Z., Liu, H., Liu, F., Lin, F., Wu, R., Zhang, R., and Lu, Q. Direct construction of a three-dimensional structure with cells and hydrogel. J Bioactive Compatible Polym **20,** 259, 2005.
27. Kuo, C.K., and Ma, P.X. Ionically crosslinked alginate hydrogels as scaffolds for tissue engineering: part 1. Structure, gelation rate and mechanical properties. Biomaterials **22,** 511, 2001.
28. Gleghorn, J.P., Jones, A.R., Flannery, C.R., and Bonassar, L.J. Boundary mode frictional properties of engineered cartilaginous tissues. Eur Cells Mater **14,** 20, 2007.
29. Gleghorn, J.P., Lee, C.S., Cabodi, M., Stroock, A.D., and Bonassar, L.J. Adhesive properties of laminated alginate gels for tissue engineering of layered structures. J Biomed Mater Res Part A **85,** 611, 2007.
30. Lee, C.S., Gleghorn, J.P., Choi, N.W., Cabodi, M., Stroock, A.D., and Bonassar, L.J. Integration of layered chondrocyte-seeded alginate hydrogel scaffolds. Biomaterials **28,** 2987, 2007.
31. Malone, E., and Lipson, H. Fab@Home: the personal desktop fabricator kit. Rapid Prototyping J **13,** 245, 2007.
32. Genes, N.G., Rowley, J.A., Mooney, D.J., and Bonassar, L.J. Effect of substrate mechanics on chondrocyte adhesion. Arch Biochem Biophys **422,** 161, 2004.
33. Endres, M., Hutmacher, D.W., Salgado, A.J., Kaps, C., Ringe, J., Reis, R.L., Sittinger, M., Brandwood, A., and Schantz, J.T. Osteogenic induction of human bone marrow-derived mesenchymal progenitor cells in novel synthetic polymer-hydrogel matrices. Tissue Eng **9,** 689, 2003.
34. Xie, B., Parkhill, R.L., Warren, W.L., and Smay, J.E. Direct writing of three-dimensional polymer scaffolds using colloidal gels. Adv Funct Mater **16,** 1685, 2006.
35. Lam, C.X.F., Mo, X.M., Teoh, S.H., and Hutmacher, D.W. Scaffold development using 3D printing with a starch-based polymer. Mater Sci Eng Part C **20,** 49, 2002.
36. Rüdiger, L., and Rolf, M. Desktop manufacturing of complex objects, prototypes and biomedical scaffolds by means of computer-assisted design combined with computer-guided 3D plotting of polymers and reactive oligomers. Macromol Mater Eng **282,** 17, 2000.
37. Vozzi, G., Flaim, C., Ahluwalia, A., and Bhatia, S. Fabrication of PLGA scaffolds using soft lithography and microsyringe deposition. Biomaterials **24,** 2533, 2003.
38. Vozzi, G., Previti, A., De Rossi, D., and Ahluwalia, A. Microsyringe-based deposition of two-dimensional and three-dimensional polymer scaffolds with a well-defined geometry for application to tissue engineering. Tissue Eng **8,** 1089, 2002.
39. Weinand, C., Pomerantseva, I., Neville, C.M., Gupta, R., Weinberg, E., Madisch, I., Shapiro, F., Abukawa, H., Troulis, M.J., and Vacanti, J.P. Hydrogel-[beta]-TCP scaffolds and stem cells for tissue engineering bone. Bone **38,** 555, 2006.
40. Shor, L., Guceri, S., Gandhi, M., Wen, X., and Sun, W. Solid freeform fabrication of polycaprolactone/hydroxyapatite tissue scaffolds. J Manufact Sci Eng **130,** 210, 2008.
41. Wang, F., Shor, L., Darling, A., Khalil, S., Sun, W., Guceri, S., and Lau, A. Precision extruding deposition and characterization of cellular poly-caprolactone tissue scaffolds. Rapid Prototyping J **10,** 42, 2004.
42. Xiong, Z., Yan, Y., Wang, S., Zhang, R., and Zhang, C. Fabrication of porous scaffolds for bone tissue engineering via low-temperature deposition. Scr Mater **46,** 771, 2002.

43. Nair, K., Yan, K., and Sun, W. A computational modeling approach for the characterization of mechanical properties of 3D alginate tissue scaffolds. J Appl Biomater Biomech **6,** 35, 2008.
44. Chang, R., Nam, J., and Sun, W. Effects of dispensing pressure and nozzle diameter on cell survival from solid freeform fabrication-based direct cell writing. Tissue Eng Part A **14,** 41, 2008.
45. Li, M., Tian, X., Zhu, N., Schreyer, D.J., and Chen, X. Modeling process-induced cell damage in the biodispensing process. Tissue Eng Part C Methods **16,** 533, 2010.

Address correspondence to:
Lawrence J. Bonassar, Ph.D.
Department of Mechanical and Aerospace Engineering
Cornell University
149 Weill Hall
Ithaca, NY 14853

E-mail: lb244@cornell.edu

Received: February 11, 2010
Accepted: September 7, 2010
Online Publication Date: November 30, 2010